Permeation Rates of Oxygen through a Lipid Bilayer using Replica Exchange Transition Interface Sampling

Enrico Riccardi,[†] Andreas Krämer,[‡] Titus S. van Erp,[†,¶] and An Ghysels[*,§]

†*Department of Chemistry, Norwegian University of Science and Technology, Høgskoleringen 5, 7491 Trondheim, Norway*

‡*Laboratory of Computational Biology, National Heart, Lung, and Blood Institute, National Institutes of Health, Bethesda, Maryland 20892, United States*

¶ *Center for Molecular Modeling (CMM), Ghent University, Technologiepark, Zwijnaarde, Belgium*

§*IBiTech, Faculty of Engineering and Architecture, Ghent University, Corneel Heymanslaan 10, Block B - entrance 36, 9000 Gent, Belgium*

E-mail: an.ghysels@ugent.be

Abstract

Several simulations strategies have emerged to predict the permeability of solutes across membranes, which is important for many biological or industrial processes such as drug design. The wide-spread inhomogeneous solubility-diffusion (ISD) model is based on the Smoluchowski equation and describes permeation as purely diffusive. The counting method, which counts membrane transitions in a long molecular dynamics (MD) trajectory, is free of this diffusive assumption, but it lacks sufficient statistics when the permeation involves high free energy barriers. Metadynamics and variations thereof can overcome such barriers, but they generally lack the kinetics information. The milestoning framework has been used to describe permeation as a rare event, but it still relies on the Markovian assumption between the milestones. Replica Exchange Transition Interface Sampling (RETIS) has been shown to be an effective method for sampling rare events while simultaneously describing the kinetics without assumptions. This paper is the first permeation application of RETIS on an all-atom lipid bilayer consisting of 1-palmitoyl-2-oleoyl-sn-glycero-3-phosphocholine (POPC) to compute the entrance, escape and complete transition of molecular oxygen. Conventional MD was performed as a benchmark, and the MD rates from counting were converted to rate constants, giving good agreement with the RETIS values. Moreover, a correction factor was derived to convert the collective order parameter in RETIS, which was aimed to improve efficiency, to a single-particle order parameter. With this work, we showed how the exact kinetics of drug molecules permeation can be assessed with RETIS even if the permeation is truly a rare event or if the permeation is non-Markovian. RETIS will therefore be a valuable tool for future permeation studies.

Introduction

Permeation of compounds is essential for the biology of cells and organelles. Where experiments often miss the details of transport at the atomic scale, such as the inhomogeneity and anisotropy of phospholipid membranes, computational studies can give this detailed

insight. In molecular dynamics (MD), trajectories of the permeants are created that give explicit information on the transport properties. An example is the passive transport of small molecules through a series of phospholipid bilayers[1–6] for which Bayesian analysis (BA) based on the Smoluchowski equation could provide the permeability with reasonable computational cost.[7] Another approach is the counting method, where direct counting of membrane crossings observed in the MD trajectories gives the permeability.[7–10]

However, when the membrane crossings are a rare event, conventional MD might not reach long enough time scales to obtain sufficient statistics for the BA nor the counting method.[10,11] In the case of a high membrane barrier, there are numerous enhanced sampling methods that aim at constructing the free energy profile across the membrane,[12,13] but these methods often lack information on the kinetics. Some recent studies, therefore, relied on the milestoning algorithm to compute the membrane crossing rate.[14–17] A disadvantage of milestoning is that the kinetics between milestones is assumed to be Markovian.

Recently, Replica Exchange Transition Interface Sampling (RETIS)[18,19] has been put forward as a method that can sample rare permeation events while simultaneously describing the kinetics without diffusive assumptions. In the present paper, the RETIS framework will be used for the first time to treat the transport kinetics of small molecules through an all-atom phospholipid bilayer consisting of thousands of particles. In RETIS, the transition from a reactant to a product state is divided in multiple subsequent steps (interfaces), where the probability to reach the next step is measured. In this divide-and-conquer approach, the overall crossing probability is expressed as a product of probabilities that paths in the i-th path ensemble, denoted $[i^+]$, reach the next interface $i+1$. The path ensemble $[i^+]$ contains all paths that start at interface 0, end at interface 0 or at the last interface, and cross interface i at least once. The paths are collected via a detailed-balance Monte Carlo (MC) procedure such that one obtains a statistical distribution as if they are cut out from an endlessly long MD trajectory. By evaluating the series of conditional probabilities to reach interface $i+1$ given interface i is reached from interface 0, one can evaluate the very small probability

that the last interface is reached after a crossing with interface 0, i.e. the overall crossing probability. The conditional crossing probabilities are much larger such that only relatively few paths in the respective path ensembles are needed to evaluate them. RETIS has one additional path ensemble $[0^-]$, which contains all paths starting and ending at interface 0, similar to $[0^+]$, but they explore the left side of interface 0 between start and end. Hence, $[0^-]$ explores the reactant state instead of the barrier region. The rate is finally expressed by the product of the overall crossing probability and the flux, where the latter is obtained from the average path lengths in the $[0^-]$ and $[0^+]$ path ensembles.[19] This technique allows to evaluate rates that would otherwise not be accessible with currently feasible computational resources.

The framework of RETIS as a rare event method differs strongly from conventional MD. In RETIS, the path ensembles are sampled with MC moves in path space. From a given path (trajectory), a new path is generated using some MC move, and the new path is accepted or rejected according to a certain importance sampling acceptance probability. An example is the shooting move which randomly selects a phase point of the current path and then randomly changes the velocity component as if shooting away from the current trajectory. Next this new phase point is extended backwards and forwards in time to create the new path. Another example is the replica exchange move, which proposes to swap two paths belonging to different ensembles. This swap move improves the sampling efficiency in path space compared to plain Transition Interface Sampling (TIS).[18,20,21]

For the shooting move, we used aimless velocity change which implies that for the randomization of velocities, all atomic velocities are regenerated from a Maxwell-Boltzmann distribution. This provides a faster decorrelation from the previous path than the approach in which momenta are only slightly perturbed.[18] Due to detailed-balance and the aimless velocity randomization, the acceptance probability of the shooting move becomes equal to the ratio of path lengths of the old path and the new path. In practice this means that a very long path has a high probability to get rejected, which would imply wasting many MD

steps. However, to reduce unnecessary MD steps, we effectively include the acceptance step by defining a maximum allowed path length for the new path, equal to the old path length divided by an uniform random number between 0 and 1.[20] Once the new path exceeds the maximum path length, the move is immediately rejected and the old path is kept. If the path is completed within the maximum allowed path length and obeys the path ensemble's criteria, it is directly accepted. The acceptance probability of the MC moves ranged from 0.44 till 0.66 for the different path ensembles in our system.

With the aim to simulate the permeation of complex molecules through membranes in future applications, this paper will validate the estimation of the membrane crossing rate with RETIS, using the recent implementation of RETIS in the PyRETIS library.[22,23] Special attention will be given to the choice of order parameter and interfaces. As a proof of concept, the transport of O_2 through 1-palmitoyl-2-oleoyl-sn-glycero-3-phosphocholine (POPC) will be studied. This system has the advantage that the statistics on the rates for entering and escaping the membrane are sufficient with conventional MD,[10] such that the RETIS permeation rates may be compared with direct counting of membrane transitions. The outset of the paper is therefore straightforward: the oxygen permeation rates are compared between (1) a long conventional unbiased MD simulation where the counting method is applied, and (2) RETIS rare event simulations. The counting method yields rates whereas RETIS yields rate constants, and thus we also report on the steps that need to be taken to allow interpretation of the results.

The Methodology Section describes both the MD and the RETIS simulation protocols. In the Results and Discussion Section, the MD permeation rates for entrance and escape of molecular oxygen are compared to the RETIS rates. The rate of complete transitions is shown to follow from the entrance rate. The connection between rates in MD and RETIS rate constants is explained. A correction factor is derived for the escape rate, which is needed because of the order parameter choice in the present paper. The last section gives the conclusions.

Methodology

Benchmark MD simulations of POPC

A homogeneous symmetric bilayer of 72 POPC molecules was investigated with 10 permeating oxygen molecules, as shown in Fig. 1. This bilayer was found to yield fairly good statistics for membrane crossings by oxygen in previous studies[7,8,11,24–26,26] with the CHARMM software.[27] It can therefore provide the entrance and escape rates from conventional MD simulations, which will serve as the benchmark for the RETIS rates.

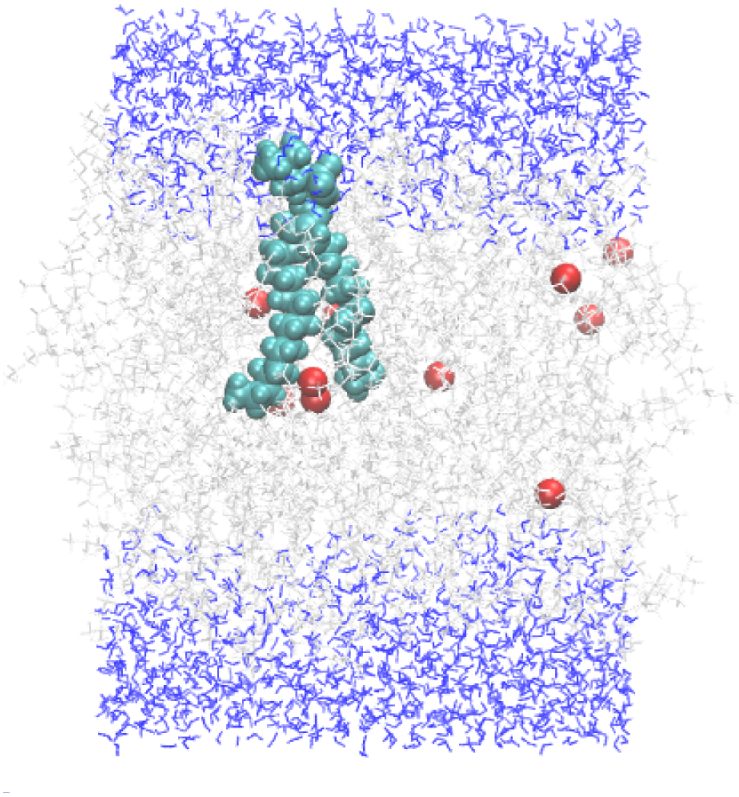

Figure 1: Simulation box of POPC membrane with 72 phospholipids (grey), a water layer (blue) and 10 O_2 molecules (red). One POPC is colored light blue.

The membrane was placed in the center of the simulation box. The water solvent layer consisted of 2242 water molecules. The box was kept tetragonal and periodic boundary conditions were applied. The MD simulations were performed with the Gromacs software[28] using the CHARMM36 lipid force field,[29] the modified TIP3P water model,[30,31] and the

interaction parameters for molecular oxygen given in the supporting information of Ref. 24. The integration time step was 1 fs, global translations of the box were removed every 0.1 ps, and the v-rescale thermostat[32] was used to control the temperature at 298 K and the Parrinello-Rahman barostat for the pressure at 1 atmosphere. After equilibration of the simulation box for 60 ns, a long equilibrium NPT run of 500 ns was produced. The average area per lipid was 64.5 Å^2 while the average box height was $L = 67.0$ Å in the z-direction orthogonal to the membrane surface.

A slight drift of the bilayer's position over time is possible because this is not prevented by the removal of the global translations. In the post-processing of the data, the center of mass of the bilayer was tracked as a function of time, $z_{\mathrm{COM}}(t)$, and the whole simulation box was shifted by $-z_{\mathrm{COM}}(t)$ at every time step. Next, the periodic boundary conditions were applied again to ensure that all permeant molecules were in the primary box. We denote these coordinate as z': they can be interpreted as the position with respect to the membrane center. The histogram of these coordinates will have blurred boundaries around $\pm L/2$ because of the fluctuating instantaneous box length $L(t)$. Instead, the coordinates are normalized with $L(t)$ and rescaled with L to obtain $z(t) = L\,z'(t)/L(t)$, which lie between $-L/2$ and $L/2$ at every time step. The histogram $p(z)$ was constructed from these z-coordinates, from which the free energy profile was derived as $F(z) = -k_B T \ln p(z)$, up to an arbitrary constant term, where T is temperature and k_B is Boltzmann's constant. Crossings through the bilayer leaflets (escape, entrance) and complete membrane transitions were detected with the Rickflow package.[26]

Set-up for RETIS

To start the RETIS simulations, two stable states A and B should be defined that play the role of reactant and product states. Based on the free energy profile of the oxygen molecules (Fig. 2), two states can be identified. The first state around $z = 0$ corresponds to the interleaflet region of the membrane (called *inside*), while the second state around $z = 3$ nm

corresponds to the solvent region (called *outside*). To quantify the oxygen transport via a

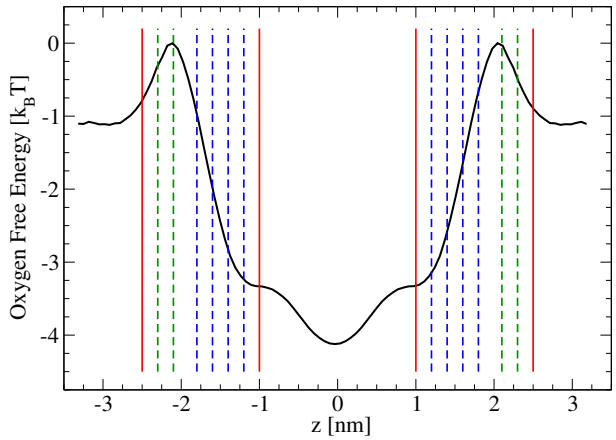

Figure 2: Free energy profile $F(z)$ (black line) of oxygen molecules along the direction orthogonal to the POPC membrane. Membrane center is located at $z = 0$. The red lines are the λ_A and λ_B interfaces; they define the two stable states: inside ($|z| < 1$ nm) and outside ($|z| > 2.5$ nm). The dashed lines show the position of the other interfaces: blue for *escape*, green for *entrance*.

kinetic theory, the rate of oxygen transits between these two stable states (inside and outside regions) has to be estimated, i.e. the rate of oxygen permeation from outside the POPC to the interleaflet region of the membrane, and vice-versa. These rates are hereon labeled as *escape* rate and *entrance* rate.

For both rates, an order parameter is used that is based on the z-coordinate of the center of mass of the O_2 molecules, where z_i refers to the i-th molecule. Similarly as described in the MD subsection, the whole simulation box was shifted to let the center of mass of the membrane coincide with $z = 0$, so z_i effectively describes center of mass separation between the i-th oxygen and the membrane center. A difference with the MD subsection is that the coordinates were not normalized by the instantaneous box length nor scaled back with the average box length.

The RETIS order parameter is different for the two rates. For the entrance rate, assuming the first oxygen molecule is selected as the target permeant, the order parameter is defined as

$$\lambda = -|z_1| \tag{1}$$

which represents the absolute distance of the selected oxygen molecule with respect to the center of mass of the membrane. For the escape rate, we aimed to increase the sampling efficiency by selecting 5 target permeants out of the 10 oxygen molecules. The order parameter is defined as

$$\lambda = \max_{i \in \{1,\ldots,5\}} |z_i| \tag{2}$$

which represents the largest absolute distance from the center of mass of the membrane of those 5 pre-selected oxygen molecules. In effect, this new order parameter for the escape rate has the same physical meaning as the entrance rate, but it will provide a rate of the event that *any* of the 5 pre-selected oxygens escapes, which is 5 times faster than the escape rate for an individual O_2 if we assume that the transition events are uncorrelated. This assumption will be checked in the Results and Discussion Section. The minus sign in the definition Eq. 1 is a purely technical aspect, since the RETIS implementation in the PyRETIS software requires the order parameter to increase from the initial state to the final state. We will therefore generally omit the minus sign in the discussion, citing $|\lambda|$ instead when referring to λ. In this text, λ is expressed in nanometers.

The absolute value in Eqs. 1 and 2 makes the order parameter a symmetrical function of z_i. It allows observation of membrane barrier crossings in both leaflets within a single RETIS simulation (see Fig. 3). For the escape, it means that the rate of exiting is computed through either the upper or lower leaflet (blue arrows), while for the entrance, the permeants can enter through either of the two leaflets (green arrows) via the periodic boundary conditions. This flexibility in considering both leaflets at once increases the efficiency of the approach.

The leaflets are defined as the regions $\lambda \in [1.0, 2.5]$. For the escape, stable state A corresponds to $\lambda < \lambda_A = 1$ and stable state B to $\lambda > \lambda_B = 2.5$. For the entrance, the role of λ_A and λ_B are reversed. The RETIS algorithm computes crossing probabilities from one side to the other and complements those with a flux calculation through the $\lambda = 1$ interface for the escape and through the $\lambda = 2.5$ interface for the entrance. In regards to the simulation set-up, the interfaces for the escape transition are located at (1.0, 1.2, 1.4, 1.6,

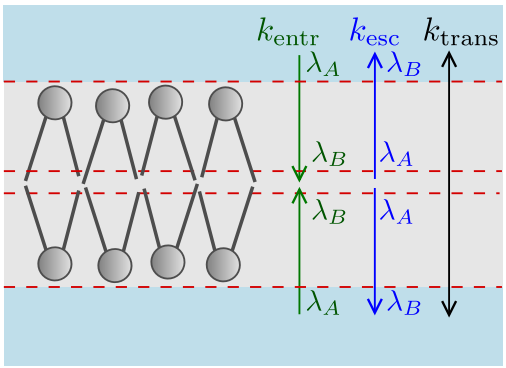

Figure 3: Schematic view of the bilayer showing the definition of the entrance and escape rate constants through the leaflets. In RETIS, the starting interface is located at λ_A and the ending interface is located at λ_B. Because of the absolute value in the definitions of λ, RETIS computes the rates through the two leaflets at once.

1.8, 2.5), while for the entrance transition the interfaces (2.5, 2.3, 2.1, 1.0) suffice. A larger density of interfaces is needed whenever the free energy profile shows a steep increase. Fig. 2 reports the free energy profile (black line) with the limits of the stable states (red lines, λ_A and λ_B interfaces). The location of the other RETIS interfaces for the escape and entrance simulations are indicated in blue and green, respectively.

For solutes other than O_2, the distinction between entrances, escapes, and complete transitions in Fig. 3 might not be useful. For H_2O, for instance, the membrane represents a high free energy barrier of over $10\,k_BT$, leading to a short residence time in the membrane center. For such permeants, only the rate of complete transitions would be computed by placing the RETIS interfaces on the barrier's slope.

For both path sampling simulations, the probability of swap moves (replica exchange moves between path ensembles), time reversal moves and shooting moves was set to 0.5, 0.25, and 0.25, respectively. The order parameter was computed by PyRETIS based on the Gromacs coordinates every 100 MD integration steps performed by Gromacs, so every 0.1 ps. Each path ensemble contained 18 500 to 19 200 paths.

Results and Discussion

Direct observation of rates in conventional MD

The free energy profile $F(z)$ across the membrane in Fig. 2 is derived from the histogram of the MD trajectories. It has a free energy well of about 3 k_BT with respect to the water phase, indicative of the higher oxygen concentration near the bilayer midplane than in the water phase. This higher partitioning of oxygen in the membrane is in accordance with earlier simulations at 298 K.[25] To exit the membrane center, O_2 should escape over a barrier of approximately $4\,k_BT$. When in the water phase, O_2 should cross a smaller barrier of about $1\,k_BT$ to enter the membrane. The location of the barrier is at about $z_{\max} = 2.1$ nm from the bilayer midplane.

The number of escapes, entrances and complete transitions can be directly observed in the conventional MD simulations by detecting the transitions in the oxygen trajectories. This is referred to as the counting method in earlier work on permeability calculations of oxygen and water through phospholipid bilayers, where the focus was on complete membrane crossings events.[7,10,11] In this work, also the escape events from the membrane center and entrance events into the membrane are detected. The dividing surfaces that define an entrance or escape are the $z = \pm 2.5$ nm planes (outside) and $z = \pm 1$ nm planes (inside), similarly to the two stable states of the RETIS simulations. Complete membrane crossings between the $z = \pm 2.5$ nm dividing surfaces are referred to as *transitions* (Fig. 3).

Table 1: Entrance, escape and complete transitions from the MD simulations using the counting method: detected numbers by the 10 O_2 molecules and rate r with its C.I. Overall state probability p_A is estimated with $p_{\mathbf{out}}$ (entrance, transition) and $p_{\mathbf{in}}$ (escape). Last columns contain rate constant k (Eqs. 4, 6) with C.I. estimated as a percentage (error on p_A not taken into account).

	count	r ns^{-1}	C.I.(r) ns^{-1}	$p_{\mathrm{out/in}}$	k ns^{-1}	C.I.(k)
entrance	68	0.0136	(0.0104-0.0170)	0.058	0.234	($\pm$25%)
escape	70	0.0140	(0.0108-0.0174)	0.942	0.0149	($\pm$24%)
transition	36	0.0072	(0.0050-0.0096)	0.058	0.124	($\pm$33%)

The counts of the events in Table 1 are observed over the duration of $T_{\text{sim}} = 500$ ns, where all 10 oxygen molecules were considered. The conversion from the entrance count N_{entr} to the entrance rate reads

$$r_{\text{entr}} = \frac{N_{\text{entr}}}{N_p \, T_{\text{sim}}} \tag{3}$$

with N_p the number of permeating molecules. The escape rate r_{esc} and transition rate r_{trans} have similar definitions. These definitions differ from the previously used rate definitions which had an additional division by the unit cell cross area A_{xy},[7,11] because in this paper we aspire comparison with RETIS rates, which have inverse time as unit, rather than the unit of molecules per area per time.

In Table 1, the escape or entrance rates are approximately equal. This is easily understood when realizing that the MD simulations occurred in thermodynamic equilibrium, where the total flux of particles necessarily is overall equal to zero. Therefore, an equal number of particles has to leave the membrane as the number of particles that enter the membrane, to avoid a concentration buildup in the membrane, and hence $r_{\text{entr}} = r_{\text{esc}}$ in a long equilibrium run.

To convert rates to rate constants, the rates are divided by the probability of the overall state $p_{\mathcal{A}}$.[20,33] The need for this conversion comes from the different mindset of observed rates and rate constants. A rate constant describes the kinetics of making a crossing given that it is in a particular state. The observed rates do not take into account the condition of being in a particular overall state. The condition can therefore be introduced by division by the probability to be either inside or outside. For escape and entrance, this is $p_{\mathcal{A}} = p_{\text{in}}$ and $p_{\mathcal{A}} = p_{\text{out}}$, respectively, giving

$$k_{\text{esc}} = \frac{r_{\text{esc}}}{p_{\text{in}}}, \quad k_{\text{entr}} = \frac{r_{\text{entr}}}{p_{\text{out}}} \, . \tag{4}$$

Here, p_{out} and p_{in} are associated to the *overall* states instead of the stable states.[18] Hence, p_{out} is the probability that O_2 was last outside the membrane with $|z| > 2.5\,\text{Å}$ and has

not entered the membrane center region $|z| < 1\,\text{Å}$ yet. The definition of p_{in} is similarly the probability that O_2 was last inside the membrane without having fully escaped the membrane yet. In practive, p_{out} and p_{in} follow from integrating the probability histogram over $|z| > z_{\max}$ and $|z| < z_{\max}$ with $z_{\max}$=2.1 nm corresponding to the maximum of the free energy curve (see Fig. 2) giving the values in Table 1. One should note that generally $k_{\text{esc}} \neq k_{\text{entr}}$, since usually $p_{\text{in}} \neq p_{\text{out}}$.

The isolated event of entering the membrane takes about 0.5 ns.[34] Compared to the average time between events, which equals $T_{\text{sim}}/N_{\text{entr}} = 6.7$ ns, a membrane entrance can be regarded as a limiting case of a rare event. Consequently, the waiting time distribution between entrances can be regarded as a Poisson process. The same principle holds for the escape events. The confidence intervals on the counts are estimated using the Poisson distribution and are converted to 95-% confidence intervals (C.I.) for the rates (Table 1).[26] The average time between events involves the exploration of the stable states and failed attempts to cross the barrier. In rare events, this time is generally orders of magnitude larger than the transition time duration, the time to cross the barrier once the transition is initiated.[21] In this situation it is 'just' one order of magnitude larger which makes the oxygen permeation through the POPC membrane a borderline rare event case.

Rates of complete transitions

In the specific case of oxygen permeation through the POPC membrane, the equilibrium condition moreover makes it possible to derive the rate r_{trans} of complete transitions from the entrance or escape rate. O_2 molecules get temporarily trapped near the midplane of the bilayer, for a time span of on average approximately 50 ns.[34] This is ample time to randomize the velocity of an O_2 molecule, and it will randomly escape the membrane either towards the membrane border through which it entered, either towards the other side, with equal probability 1/2. The (bidirectional) transition rate is therefore equal to half of the escape

and entrance rates,

$$r_{\text{trans}} = \frac{r_{\text{entr}}}{2} = \frac{r_{\text{esc}}}{2} \tag{5}$$

which is confirmed by the data in Table 1. This is indeed true for molecular oxygen permeation through POPC, while it is not necessarily valid for other permeants.[26] Following the reasoning of Eq. 4, the transition rate is converted to a rate constant by division through p_{out},

$$k_{\text{trans}} = \frac{r_{\text{trans}}}{p_{\text{out}}} = \frac{k_{\text{entr}}}{2} \tag{6}$$

showing that the transition rate constant is equal to half the entrance rate constant. Note that we cannot replace k_{entr} in Eq. 6 by its 'escape counterpart' like in Eq. 5 as generally $k_{\text{entr}} \neq k_{\text{esc}}$ (see Eq. 4).

Comparison with rates from transition interface sampling

The rate constants of rare events that occur on a timescale beyond that what is accessible by conventional MD can be computed by TIS and RETIS. The (RE)TIS approaches express the rate constant k_{AB} as a flux f_A through an interface λ_A close to the reactant state A times the crossing probability $P_A(\lambda_A|\lambda_B)$,

$$k_{AB} = f_A P_A(\lambda_A|\lambda_B)\,. \tag{7}$$

The crossing probability $P_A(\lambda_A|\lambda_B)$ is the probability that after crossing λ_A, another interface λ_B is crossed before another λ_A crossing. Interface λ_B is placed close to the product state. As previously discussed, to study the transport of oxygen, the entrance transition and the escape transition have been sampled. For the entrance, the reactant and product state are the state where the target permeant is outside and inside the membrane, respectively. For the escape, the reactant and product state are reversed with the additional notion that the resulting permeant can be any of the 5 pre-selected permeants defining the reaction

coordinate (Eq. 2). For the complete transitions, no RETIS simulation was performed. We can link the transition probability to the entrance probability, because once O_2 is in the membrane, it has a probability of approximately 1/2 to exit to either side (see above). Compared to the entrance rate constant, the crossing probability is divided by a factor two and the flux remains unchanged, and thus Eq. 6 was used to derive k_{trans} from the RETIS value for k_{entr}.

Table 2 shows the crossing probability $P_A(\lambda_A|\lambda_B)$ and the flux f_A for the entrance and escape. The C.I. can be estimated by taking twice the reported standard error. The transition

Table 2: RETIS crossing probability, flux and rate constant for entrance, escape and complete membrane transitions. First two lines are direct results from RETIS simulations. Third line contains correction factors, giving the corrected escape (1) quantities. Standard errors (s.e.) between brackets from block averaging; standard errors for escape (1) is an underestimation as it does not take into account the error on the correction factors.

	$P_A(\lambda_B\|\lambda_A)$	s.e.	f_A ns^{-1}	s.e.	k_{AB} ns^{-1}	s.e.
entrance	4.47×10^{-3}	(±20%)	72.1	(±6%)	0.322	(±21%)
escape (max{5})	9.88×10^{-4}	(±17%)	81.7	(±12%)	0.0807	(±21%)
escape corr. factor	0.285		0.589		0.168	
escape (1)	2.81×10^{-4}	(±17%)	48.1	(±12%)	0.0135	(±21%)
transition	2.24×10^{-3}	(±20%)	72.1	(±6%)	0.161	(±21%)

rate constants, which are ultimately linked to the membrane permeability, of the RETIS and MD simulations are comparable, 0.161 ns^{-1} (±42%) and 0.124 ns^{-1} (±33%), respectively. Given the large C.I., there is no statistically significant difference between the two results. Note again that the escape rate is not needed to determine the transition rate constant, but the latter is solely based on the entrance rate constant. The escape rate in RETIS is not directly comparable to MD results due to the chosen RETIS order parameter, Eq. 2, that depends on the maximum displacement from the center of 5 pre-selected permeants. The RETIS escape rate constant therefore needs a correction factor to obtain the 1-particle rate constant that is assessed in MD.

For truly rare events, the correction for obtaining the escape rate for a single particle

from a 5-particle rate is trivial. For instance in Ref. 35 the dissociation of liquid water was studied by taking the maximum of all OH-bonds in the system. The initial flux in that study measured the relatively rare event of an OH stretch beyond 1.07 Å. The related crossing probability measured the chance that such a stretch leads to a full dissociation event. The trajectories describing the event after the 1.07 Å stretch, either leading to a dissociation with an extremely small probability or to a state in which non of the OH bonds is any longer overstretched, are very short (up to 1 ps). The chance, that during that time window size another uncorrelated OH stretch beyond 1.07 Å takes place, can be ignored. Therefore, in this case the frequency of OH stretches beyond 1.07 Å for one particular bond can be obtained by taking the RETIS flux, measuring the frequency of events in which *any* bond in the system stretches beyond 1.07 Å, and dividing this flux by the number of bonds in the system. The crossing probability is not changed.

In this work, however, the event is not that rare (as it can be studied by MD) and the transition events are not that short. The flux correction is therefore not a simple division by 5, since not all crossings of the first interface by the five selected ones are counted when the reaction coordinate is based on the maximum of z-values. In addition, the crossing probability based on the maximum of 5 permeants will be an overestimation compared to the single-permeant crossing probability. The following two subsections derive the correction factors needed for the escape flux and escape crossing probability.

Correction for escape flux

In order to compute the escape rate constant based on a single permeant, we will make the assumption of independent migration of the 5 permeants. For O_2 this has been found to be a valid assumption in previous work.[24,34] No statistically relevant correlation between the distance of the atoms from the center of the POPC membrane has been observed. For the analysis, the correlation matrix based on Pearson's correlation coefficients and PyVisA has

been used.[36] The unconditional flux $f^{(1)}$ for a single permeant can be expressed as

$$f^{(1)} = \frac{p(|z_1(t)| < \lambda_A \wedge |z_1(t+\Delta t)| > \lambda_A)}{\Delta t} \tag{8}$$

Here, the subindex (1) refers to the use of a single permeant, and Δt is the time interval at which the order parameter is measured. In our case this equals 100 MD steps or $\Delta t = 0.1\,\mathrm{ps}$. The interface $\lambda_A = 1$ limits *stable* state A for the escape transition. The $p(\cdot)$ probability in the numerator relates to the chance to observe a crossing with this λ_A interface from inside ($\lambda < \lambda_A$ at time t) to outside ($\lambda > \lambda_A$ at time $t + \Delta t$), where t is an arbitrary time.

The flux f_A in the RETIS expression is the conditional flux. This implies that f_A is the number of crossing events divided by the time that the system is in *overall* state $\mathcal{A}$. The system is part of the overall state $\mathcal{A}$ whenever the $\lambda_A = 1$ interface was more recently crossed than the $\lambda_B = 2.5$ interface.[18] The overall state $\mathcal{A}$ is, hence, substantially larger than the stable state A, and will extend beyond λ_A, generally close to the maximum of the free energy curve. Therefore, we assume that $p_{\mathcal{A}} = p_{\mathrm{in}} = p(|z| < z_{\max}) = 0.942$ for the escape (see Table 1). We can, henceforth, write for the conditional flux:

$$f_A^{(1)} = \frac{p(|z_1(t)| < \lambda_A \wedge |z_1(t+\Delta t)| > \lambda_A)}{\Delta t p_{\mathrm{in}}}\,. \tag{9}$$

Next, the crossing of $\lambda_A = 1$ by the maximum displacement from the center of 5 pre-selected permeants (Eq. 2) is considered. It should be noted that this corresponds to the crossing of any of the 5 permeants with the λ_A interface under the condition that the remaining 4 permeants are in the inner region ($\lambda < \lambda_A$). Hence, this flux through λ_A is

$$\begin{aligned} f^{(\max\{5\})} &= \sum_{i=1}^{5} \frac{p(|z_i(t)| < \lambda_A \wedge |z_i(t+\Delta t)| > \lambda_A) \prod_{j=1, j\neq i}^{5} p(|z_j(t)| < \lambda_A)}{\Delta t} \\ &= 5\frac{p(|z_1(t)| < \lambda_A \wedge |z_1(t+\Delta t)| > \lambda_A) p_{\mathrm{core}}^4}{\Delta t}\,. \end{aligned} \tag{10}$$

Here, $p_{\mathrm{core}} = p(|z| < \lambda_A) = 0.719$ as estimated from the probability histogram $p(z)$.

To compute the conditional flux, we should also take into account that the definition of the overall state $\mathcal{A}$ is changed due to the definition of the reaction coordinate being a maximum z-coordinate of 5 permeants. If only one of the 5 permeants exits the membrane, the system is assigned to overall state $\mathcal{B}$. Reversely, in order to be part of overall state $\mathcal{A}$, all 5 permeants must be in the membrane region. Hence, we can henceforth approximate $p_{\mathcal{A}} \approx p_{\text{in}}^5$ and write for the conditional flux:

$$f_A^{(\max\{5\})} = 5\frac{p(|z_1(t)| < \lambda_A \wedge |z_1(t+\Delta t)| > \lambda_A)p_{\text{core}}^4}{\Delta t p_{\text{in}}^5} \tag{11}$$

Comparing Eq. 11 with Eq. 9, we see that the intended $f_A^{(1)}$ can be obtained by multiplying the flux based on 5 permeants with the correction factor $p_{\text{in}}^4/(5p_{\text{core}}^4) = 0.942^4/(5 \times 0.719^4) = 0.589$.

Correction for escape crossing probability

The 5-particle crossing probability is higher than the 1-particle crossing probability. Assume that one of the 5 pre-selected permeants crosses the λ_A interface initially. In a 1-particle crossing simulation, the trajectory would be ended if this entry permeant falls back to λ_A, and this trajectory would be registered as an unsuccessful attempt to cross the barrier. In a 5-particle crossing probability, the trajectory would not necessarily be ended when the entry permeant recrosses the λ_A interface. Indeed, if the entry permeant is not too quickly recrossing λ_A again, there is a decent time window in which one of the 4 other selected permeants can cross the λ_A interface as well and take over as the leading particle with the maximum z-coordinate (Eq. 2). If that happens, then even if the entry permeant falls back, the trajectory is continued until all 5 permeants are back in the core region ($\lambda < \lambda_A$) or until one of the 5 reaches the λ_B interface. In fact, a cascade of λ_A crossings by alternating permeants might occur such that for a long time at least one of the permeants is outside the core region while none of the five are crossing the λ_B interface nor all five are getting inside

the core again simultaneously.

By analyzing all $\lambda_A \to \lambda_B$ trajectories, we obtain a correction factor equal to the fraction of direct crossings. We identify a direct crossing whenever the permeant crossing the λ_A interface at the start of the trajectory (the entry permeant) is also the permeant that crosses the λ_B interface at the end of the trajectory (exit permeant) *and* if that permeant had no recrossings with λ_A during that trajectory.

In the collected $\lambda_A \to \lambda_B$ trajectories, we observed 833 trajectories in which the entry permeant at λ_A was the same as the exit permeant at λ_B. In 373 cases, however, this permeant had at least two recrossings with λ_A. This means that there were $833 - 373 = 460$ direct crossings. In 780 trajectories, the exit permeant was different from the entry permeant. This yields a correction factor equal to $(833 - 373)/(833 + 780) = 0.285$.

Discussion of corrected escape rate

Taking the product of the two correction factors yields an overall correction of $0.589 \times 0.285 = 0.168$ for the escape rate constant. Using here the C.I. in percentage between brackets, it can be seen that the corrected rate constant of 0.0135 ns^{-1} ($\pm 42\%$) (Table 2) is in reasonable agreement with the MD result that equals 0.0149 ns^{-1} ($\pm 24\%$) (Table 1). It also found that the overall correction (0.168) to the rate constant is not so far off from the normal procedure used in truly rare events, where the flux would simply be divided by 5 and the crossing probability taken as it is (yielding an overall correction of $1/5 = 0.2$).

In retrospect, it would have been advantageous if the interface $\lambda_A = 1$ would have been positioned further away from the membrane center. As suggested in Ref. 37, the first interface should be placed such that the stable state region ($\lambda < \lambda_A$) will cover about 80% of the overall state $\mathcal{A}$ ($\lambda < z_{\max}$). For a 1-particle order parameter, the combination of stable state probability $p_{\text{core}} = 0.719$ and overall state probability $p_{\text{in}} = 0.942$ is close to this desired optimum. Unfortunately, for the 5-particle order parameter, the probability of the stable state is based on all 5 permeants being simultaneously lower than λ_A, which is only about

$p^5_{\text{core}} = 0.192$. We therefore assume that our parameter settings were not optimal for studying this transition that can be categorized as rare but not extremely rare. Comparison of the error bars even shows that the RETIS simulations achieved lower accuracy for the permeation rate constants than the BA could achieve for permeabilities in previous work,[24,26,34] which is influenced by both simulation duration and the parameter settings.

Fig. 4 shows the average path length in the different path ensembles for the entrance

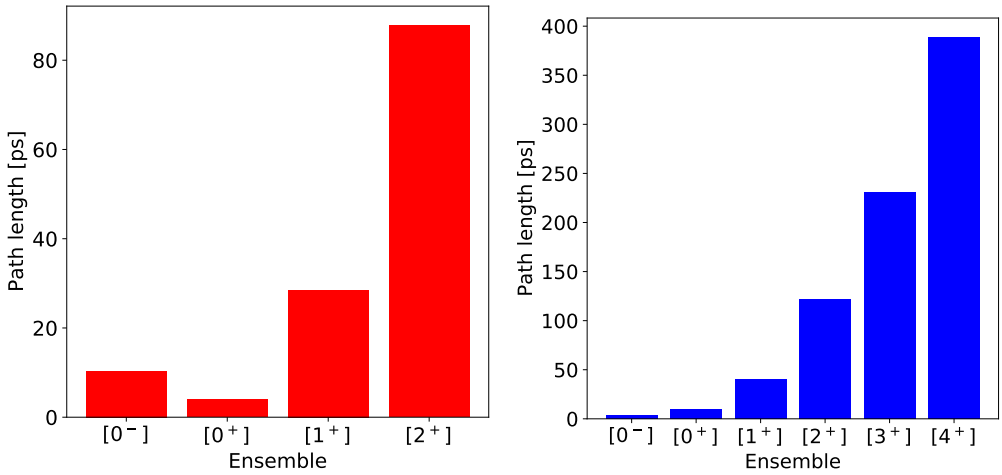

Figure 4: Average path length in RETIS simulations as a function of path ensembles for the entrance (left) and escape (right).

and escape. For the escape, it can be seen that the $[0^+]$ average path length is about a factor 3 higher than for $[0^-]$. Shifting the λ_A interface further away from the membrane center would have moved the ratio towards the expected optimum in which the $[0^-]$ paths are approximately a factor 4 longer than $[0^+]$. As an additional advantage this would also have lead to a reduced path length in all other path ensembles $[i^+], i = 1 \ldots$, since most of the paths in each ensemble start and end at λ_A. A more elaborate efficiency analysis and design for a parameter optimization protocol is planned for a future publication. We also report on a method of how to use just a single-permeant based order parameter, while still profiting from the presence of multiple permeants in the system that can be used to explore transition pathways.[38]

We further mention that in these types of very slowly diffusive dynamics, where the

transit time through the membrane is long, a change from RETIS to partial path TIS (PPTIS)[39] could probably be considered where part of the path history is neglected. Both RETIS and PPTIS has similarities with milestoning[14] that has been used before to study permeation before.[15,16] Milestoning, however, assumes full memory loss when the system hits the next interface/milestone unlike RETIS and PPTIS which incorporate, respectively, full and partial history in the condition of the conditional crossing probabilities. The memory effect vanishes and milestoning becomes exact if the interfaces/milestones are placed at iso-committor surfaces,[40] which is considered as the ideal reaction coordinate. This ideal reaction coordinate should account for all relevant rotations of the permeant, collective motions, and deformations of the membrane that could be vital for the permeation process.[38] The design of such a committor-based reaction coordinate is highly non-trivial which makes it advantageous to use a RETIS or PPTIS formalism since RETIS is exact regardless the chosen reaction coordinate and PPTIS can be made more and more exact by including more memory when the distance between interfaces is increased.

Another promising approach is the novel MC scheme of stone-skipping and web-throwing that has shown to an order of magnitude faster than RETIS based on shooting.[41] Using a reweighting technique, the MC moves show a nearly 100% acceptance while also decorrelating trajectories much more rapidly than standard shooting. The advantage of that approach is that it is only altering the MC sampling of the RETIS approach and not the path ensembles themselves as in PPTIS, and as such, the approach remains exact.

Alternative comparison between MD and RETIS

The connection between rates (MD) and rate constants (RETIS) in Eq. 4 can also be performed without needing to explicitly estimate the overall state probabilities p_{in} and p_{out}. In thermodynamic equilibrium, the rates are equal, $r_{\mathrm{entr}} = r_{\mathrm{esc}}$, which is equivalent to a detailed balance relation: $p_{\mathrm{out}}k_{\mathrm{entr}} = p_{\mathrm{in}}k_{\mathrm{esc}}$. From this relation it follows that the ratio of

probabilities is equal to a ratio of rate constants, which we call R,

$$\frac{p_{\text{out}}}{p_{\text{in}}} = \frac{k_{\text{esc}}}{k_{\text{entr}}} = R\,. \tag{12}$$

The ratio R can be computed from the RETIS 1-particle rate constants. Using R and $p_{\text{out}} + p_{\text{out}} = 1$, the overall state probabilities can be estimated as $p_{\text{in}} = 1/(1+R)$ and $p_{\text{out}} = R/(1+R)$. Finally, the MD rate of crossings through the leaflets can be predicted based on the RETIS 1-particle rate constants only,

$$r_{\text{esc}} = r_{\text{entr}} = \frac{k_{\text{entr}} k_{\text{esc}}}{k_{\text{entr}} + k_{\text{esc}}}\,. \tag{13}$$

In Table 1, conventional MD gives an entrance rate of 0.0136 ns^{-1} ($\pm 25\%$) and an escape rate of 0.0140 ns^{-1} ($\pm 24\%$), which are about equal as discussed before. Using the RETIS rate constants of Table 2 and error propagation for the C.I., the rate in Eq. 13 is 0.0130 ns^{-1} ($\pm 40\%$), which is again not statistically different from the MD result.

Conclusion

This paper is the first application of RETIS on a permeation problem with an all-atom phospholipid bilayer. The obtained rate constants are in good agreement with conventional MD. With this proof of principle at hand we have paved the way for other permeation cases in which MD is not an option. The exact kinetics of drug molecules permeation can be accessed with RETIS even if the permeation is a truly rare event or if the permeation is non-Markovian.

Moreover, the RETIS path ensembles contain trajectories that are completely physical. Unlike biased simulations where spurious effects cannot be guaranteed to be absent,[13] the RETIS trajectories can be analyzed[42] in a post-processing step, allowing to unravel the permeation process. This can be especially useful when the permeant is flexible or exhibiting

an internal degree of freedom that assists in the permeation.

In this exploratory study, we identified some key elements that should be taken into account in future permeation studies. For instance, the positioning of the first interface should be optimized when using a collective (here 5-particle) order parameter, which could substantially improve the efficiency. The design of a new protocol for choosing algorithm parameters in diffusive systems will therefore be part of our future publications. Moreover, we mentioned several existing techniques and new developments that are in progress, which will facilitate the sampling of these kind of systems. These techniques include PPTIS,[39] stone-skipping and web-throwing,[41] and the new MC moves described in Ref. 38.

In terms of efficiency, RETIS was demonstrated to efficiently sample rare events that are inaccessible with MD in the past, where it was most advantageous for extreme rare events with short transition pathways. In this study, the total number of MD steps performed in the RETIS path ensembles corresponded to 1.4 microseconds, while in the regular MD simulations, we have performed a 0.5 microseconds simulation. Based on the statistical errors of the rate constants, we did not necessarily obtain an improved efficiency with RETIS in comparison with MD. The reason is that we selected a system where permeation is not that rare, such that escapes and entrances could also be studied with MD. In addition, our parameter set up was in hindsight not optimal as discussed above. In membranes that involve higher barriers, RETIS is expected to easily outperform conventional MD in efficiency. With improved protocols for setting the algorithmic parameters, such as interface positions, and the development of new path generating moves[38,41] the efficiency is expected to increase even further. We therefore believe that RETIS will be a valuable tool for future permeation studies.

Acknowledgement

E.R. and T. S. v. E. thank the Research Council of Norway (project number 267669). Some of the computational resources (Stevin Supercomputer Infrastructure) and services used in this work were provided by the VSC (Flemish Supercomputer Center), funded by Ghent University, FWO and the Flemish Government – department EWI.

References

(1) Subczynski, W. K.; Pasenkiewicz-Gierula, M.; McElhaney, R. N.; Hyde, J. S.; Kusumi, A. Molecular dynamics of 1-palmitoyl-2-oleoylphosphatidylcholine membranes containing transmembrane α-helical peptides with alternating leucine and alanine residues. *Biochemistry* **2003**, *42*, 3939–3948.

(2) Ivanov, I. I.; Fedorov, G. E.; Guskova, R. A.; Ivanov, K. I.; Rubin, A. B. Permeability of lipid membranes to dioxygen. *Biochem. Biophys. Res. Commun.* **2004**, *322*, 746–750.

(3) Widomska, J.; Raguz, M.; Subczynski, W. K. Oxygen permeability of the lipid bilayer membrane made of calf lens lipids. *BBA - Biomembranes* **2007**, *1768*, 2635–2645.

(4) Möller, M. N.; Lancaster, J. R.; Denicola, A. The Interaction of Reactive Oxygen and Nitrogen Species with Membranes. *Curr. Top. Membr.* **2007**, *61*, 23–42.

(5) Möller, M. N.; Li, Q.; Chinnaraj, C.; Cheung, H. C.; Lancaster Jr., J. R.; Denicola, A. Solubility and diffusion of oxygen in phospholipid membranes. *Biochim. Biophys. Acta* **2016**, *1858*, 2923–2930.

(6) Awoonor-Williams, E.; Rowley, C. N. Molecular Simulation of Nonfacilitated Membrane Permeation. *Biochim. Biophys. Acta - Biomembr.* **2016**, *1858*, 1627–1687.

(7) Venable, R. M.; Krämer, A.; Pastor, R. W. Molecular Dynamics Simulations of Membrane Permeability. *Chem. Rev.* **2019**, 5954–5997.

(8) Dotson, R. J.; Smith, K., Bueche; Angles, G.; Pias, S. C. Influence of Cholesterol on the Oxygen Permeability of Membranes: Insight from Atomistic Simulations. *Biophys. J.* **2017**, *112*, 2336–2347.

(9) Dotson, R. J.; Pias, S. C. Reduced Oxygen Permeability Upon Protein Incorporation Within Phospholipid Bilayers. *Adv. Exp. Med. Biol.* **2018**, *1072*, 405–411.

(10) Davoudi, S.; Ghysels, A. Sampling efficiency of the counting method for permeability calculations estimated with the inhomogeneous solubility-diffusion model. *J. Chem. Phys.* **2020**, *In revision*.

(11) Ghysels, A.; Krämer, A.; Venable, R.; Teague, W.; Lyman, E.; Gawrisch, K.; Pastor, R. W. Permeability of Membranes in the Liquid Ordered and Liquid Disordered Phases. *Nat. Commun.* **2019**, *10*, 5616.

(12) Darve, E.; Pohorille, A. Calculating free energies using average force. *J. Chem. Phys.* **2001**, *115*, 9169–9183.

(13) Neale, C.; Pomès, R. Sampling errors in free energy simulations of small molecules in lipid bilayers. *Biochimica et Biophysica Acta (BBA) - Biomembranes* **2016**, *1858*, 2539–2548.

(14) Faradjian, A. K.; Elber, R. Computing time scales from reaction coordinates by milestoning. *J. Chem. Phys.* **2004**, *120*, 10880.

(15) Cardenas, A. E.; Elber, R. Computational study of peptide permeation through membrane: Searching for hidden slow variables. *Mol. Phys.* **2013**, *111*, 3565–3578.

(16) Votapka, L. W.; Lee, C. T.; Amaro, R. E. Two Relations to Estimate Membrane Permeability Using Milestoning. *J. Phys. Chem. B* **2016**, *120*, 8606–8616.

(17) Fathizadeh, A.; Elber, R. Ion Permeation through a Phospholipid Membrane: Transition State, Path Splitting, and Calculation of Permeability. *J. Chem. Theory Comput.* **2019**, *1*, 720–730.

(18) van Erp, T. S. Reaction Rate Calculation by Parallel Path Swapping. *Phys. Rev. Lett.* **2007**, *98*, 268301.

(19) Cabriolu, R.; Refsnes, K. M. S.; Bolhuis, P. G.; van Erp, T. S. Foundations and latest advances in replica exchange transition interface sampling. *J. Chem. Phys.* **2017**, *147*, 152722.

(20) van Erp, T. S.; Moroni, D.; Bolhuis, P. G. A novel path sampling method for the calculation of rate constants. *J. Chem. Phys.* **2003**, *118*, 7762–7774.

(21) Peters, B. *Reaction Rate Theory and Rare Events*; Elsevier: Amsterdam, Netherlands, 2017.

(22) Lervik, A.; Riccardi, E.; van Erp, T. S. PyRETIS: A Well-Done, Medium-Sized Python Library for Rare Events. *J. Comput. Chem.* **2017**, *38*, 2439–2451.

(23) Riccardi, E.; Lervik, A.; Roet, S.; Aarø, O.; van Erp, T. S. PyRETIS 2: An Improbability Drive for Rare Events. *J. Comput. Chem.* **2019**, *41*, 370–377.

(24) Ghysels, A.; Venable, R. M.; Pastor, R. W.; Hummer, G. Position-Dependent Diffusion Tensors in Anisotropic Media from Simulation: Oxygen Transport in and through Membranes. *J. Chem. Theory Comput.* **2017**, *13*, 2962–2976.

(25) De Vos, O.; Van Hecke, T.; Ghysels, A. Effect of Chain Unsaturation and Temperature on Oxygen Diffusion Through Lipid Membranes from Simulations. *Oxygen Transport to Tissue XL, Adv. Exp. Med. Biol.* **2018**, 399–404.

(26) Krämer, A.; Ghysels, A.; Wang, E.; Venable, R. M.; Klauda, J. B.; Brooks, B. R.;

Pastor, R. W. Membrane Permeability of Small Molecules from Unbiased Molecular Dynamics Simulations. *J. Chem. Phys.* **2020**, *153*, 124107.

(27) Brooks, B. R.; Brooks, C. L., III; Mackerell, A. D., Jr.; Nilsson, L.; Petrella, R. J.; Roux, B.; Won, Y.; Archontis, G.; Bartels, C.; Boresch, S. et al. CHARMM: The Biomolecular Simulation Program. *J. Comput. Chem.* **2009**, *30*, 1545–1614.

(28) Hess, B.; Kutzner, C.; van der Spoel, D.; Lindahl, E. GROMACS 4: Algorithms for Highly Efficient, Load-Balanced, and Scalable Molecular Simulation. *J. Chem. Theory Comput.* **2008**, *4*, 435–447.

(29) Klauda, J. B.; Venable, R. M.; Freites, J. A.; O'Connor, J. W.; Tobias, D. J.; Mondragon-Ramirez, C.; Vorobyov, I.; MacKerell, J., A. D.; Pastor, R. W. Update of the CHARMM all-atom additive force field for lipids: validation on six lipid types. *J. Phys. Chem. B* **2010**, *114*, 7830–7843.

(30) Jorgensen, W. L.; Chandrasekhar, J.; Madura, J. D.; Impey, R. W.; Klein, M. L. Comparison of simple potential functions for simulating liquid water. *J. Chem. Phys.* **1983**, *79*, 926–935.

(31) Durell, S. R.; Brooks, B. R.; Bennaim, A. Solvent-Induced Forces between Two Hydrophilic Groups. *J. Phys. Chem.* **1994**, *98*, 2198–2202.

(32) Bussi, G.; Donadio, D.; Parrinello, M. Canonical sampling through velocity rescaling. *J. Chem. Phys.* **2007**, *126*, 014101.

(33) van Erp, T.; Bolhuis, P. Elaborating transition interface sampling methods. *J. Comput. Phys.* **2005**, *205*, 157–181.

(34) De Vos, O.; Venable, R. M.; Van Hecke, T.; Hummer, G.; Pastor, R. W.; Ghysels, A. Membrane Permeability: Characteristic Times and Lengths for Oxygen and

a Simulation-Based Test of the Inhomogeneous Solubility-Diffusion Model. *J. Chem. Theory Comput.* **2018**, *14*, 3811–3824.

(35) Moqadam, M.; Lervik, A.; Riccardi, E.; Venkatraman, V.; Alsberg, B. K.; van Erp, T. S. Local initiation conditions for water autoionization. *Proc. Nat. Acad. Sci.* **2018**, *115*, E4569–E4576.

(36) Aarøen, O.; Kiær, H. A.; Riccardi, E. PyVisA: Visualization and Analysis of path sampling trajectories. *J. Comput. Chem.* **2020**,

(37) van Erp, T. S. Efficiency analysis of reaction rate calculation methods using analytical models I: The two- dimensional sharp barrier. *J. Chem. Phys.* **2006**, *125*, 174106.

(38) Ghysels, A.; Roet, S.; Davoudi, S.; van Erp, T. S. Exact non-Markovian permeability from rare event simulations. *Phys. Rev. Research* **2020**, *Submitted*.

(39) Moroni, D.; Bolhuis, P. G.; van Erp, T. S. Rate constants for diffusive processes by partial path sampling. *J. Chem. Phys.* **2004**, *120*, 4055–4065.

(40) Vanden-Eijnden, E.; Venturoli, M.; Ciccotti, G.; Elber, R. On the assumptions underlying milestoning. *J. Chem. Phys.* **2008**, *129*, 174102.

(41) Riccardi, E.; Dahlen, O.; van Erp, T. S. Fast Decorrelating Monte Carlo Moves for Efficient Path Sampling. *J. Phys. Chem. Lett.* **2017**, *8*, 4456–4460.

(42) van Erp, T. S.; Moqadam, M.; Riccardi, E.; Lervik, A. Analyzing Complex Reaction Mechanisms Using Path Sampling. *J. Chem. Theory Comput.* **2016**, *12*, 5398–5410.

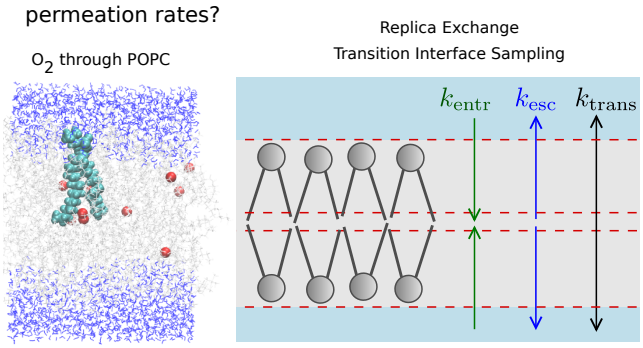

Figure 5: TOC graphic